

## ABCA Tetrablock Copolymer Vesicles

Aaron K. Brannan and Frank S. Bates\*

Department of Chemical Engineering and Materials Science,  
University of Minnesota, Minneapolis, Minnesota 55455

Received June 10, 2004

Revised Manuscript Received October 6, 2004

Self-assembly of amphiphilic molecules provides a versatile mechanism for the creation of many forms of soft materials. Lipids, soaps, and surfactants spontaneously form bilayers, cylinders, and spheres when dispersed in water, depending on the size and shape of the hydrophilic and hydrophobic portions of the molecules. Perhaps the most important of these objects is the vesicle, comprised of a thin spherical hydrophobic shell that encapsulates an aqueous medium. Living cell membranes represent the most ubiquitous and significant type of vesicle. Various block copolymer architectures (e.g., AB diblocks<sup>1–8</sup> and ABA<sup>9–11</sup> and ABC<sup>12–17</sup> triblocks) have been shown to produce the same basic morphologies found with low molecular weight amphiphiles, and polymer vesicles, also referred to as “polymerosomes”, have been targeted at drug encapsulation<sup>18–24</sup> and other biomimetic applications. Other methods to adjust micelle properties include using a triblock copolymer with a cross-linkable block, cross-linking that block in the melt, and dispersing the partially cross-linked block copolymer in a selective solvent to produce a “Janus-type” micelle with a cross-linked core and two different corona blocks.<sup>25–28</sup>

Control over the size and stability of polymer vesicles is of fundamental importance. Blending block copolymers containing different block sizes offers a promising solution to this problem.<sup>29–32</sup> Segregation of larger hydrophilic blocks to the outside surface breaks bilayer symmetry, potentially dictating spontaneous curvature and vesicle size. However, macroscopic segregation can result in multiple micelle morphologies.<sup>32</sup>

Alternatively, bilayer symmetry can be broken using architecturally asymmetric block copolymers. This communication describes our preliminary results obtained using this strategy. OSBO tetrablock copolymer vesicles were prepared with a microphase-segregated hydrophobic SB core, comprised of poly(styrene) (S) and poly(butadiene) (B) and equal length hydrophilic poly(ethylene oxide) (O) blocks. Dispersion of OSBO in water produced some degree of size control, and an unanticipated structural transition, as the fraction of O block was increased. These findings indicate that intramolecular symmetry breaking may provide a powerful tool for constructing polymerosomes with prescribed dimensions and structural features.

A set of OSBO tetrablock copolymers were prepared using a multistep synthetic procedure. A single batch of symmetric  $\alpha,\omega$ -hydroxyl-terminated HO–SB–OH diblock copolymer was produced by sequential addition of styrene and butadiene to the protected initiator 3-*tert*-butyldimethylsiloxy-1-propyllithium (FMC Lithium), followed by termination with ethylene oxide and HCl and deprotection using tetra(*n*-butyl)ammonium fluoride (TBAF). This diblock copolymer contains 51 wt % poly(styrene) and an overall molecular weight of  $M_n = 16\,200$  g/mol with polydispersity index (PDI)  $M_w/M_n =$

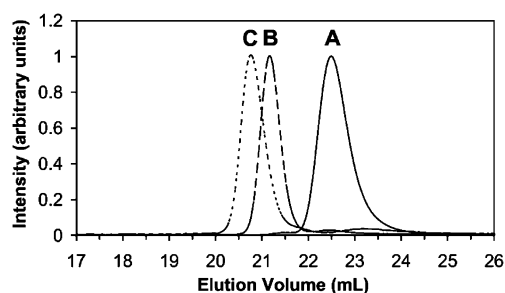


**Figure 1.** Representative normalized GPC results obtained from sample OSBO-52 during various stages of preparation: (A) S block, sampled from the reactor during polymerization, (B) SB diblock, and (C) OSBO tetrablock copolymer.

1.03, based on the reaction stoichiometry and GPC and <sup>1</sup>H NMR analyses. After recovery and purification, aliquots of this dihydroxyl-terminated diblock copolymer were reinitiated in THF with potassium naphthalenide and reacted with measured amounts of ethylene oxide, leading to the tetrablock products. Four OSBO block copolymers, containing a common parent SB core and 36, 46, 52, and 66 wt % O blocks as established by <sup>1</sup>H NMR, are the subject of this communication. We refer to these as OSBO-*w*<sub>0</sub>, where *w*<sub>0</sub> denotes the overall weight fraction of the O blocks. Figure 1 illustrates representative GPC traces obtained from the protected S block (sampled from the reactor during diblock polymerization) and SB diblock and the final OSBO product containing 52% O blocks. Overall PDI values based on GPC analysis using poly(styrene) standards ranged from 1.04 to 1.08. A combination of <sup>1</sup>H NMR end-group and GPC analyses leads us to conclude that this synthetic procedure resulted in greater than 95% tetrablock copolymer, with minor amounts of S, SB, and OS impurities. GPC results shown in Figure 1 were obtained using a Waters 410 differential refractometer with a series of three Styragel (5  $\mu$ m) columns and a flow rate of 1 mL/min. A complete summary of these synthetic methods will be published elsewhere.

Aqueous OSBO solutions were prepared by film rehydration. Approximately 0.1 g of dry polymer was dissolved in 1 mL of methylene chloride, and the solution was spread around the inside of a vial. Evaporation of the solvent left a thin film of polymer, which was dried to completion in a dynamic vacuum. 1 mL of HPLC grade water was added to each vial, and the samples were stirred at room temperature for several days, followed by several weeks at 40–50 °C. Cryo-TEM experiments at intermediate time periods were used to monitor micelle formation, which was considered to be complete when the micelles ceased to change in structure over time. Finally, solutions were diluted to roughly 0.5 wt %. At least a month of stirred hydration was required to ensure maximum dispersion of vesicles.

Tetrablock dispersions were stained by adding 100–200  $\mu$ L of 4% osmium tetroxide (OsO<sub>4</sub>) solution to 400  $\mu$ L of 0.5wt % tetrablock solutions. Within several minutes, these solutions turned from white (or clear) to brown. Stained solutions were held for 4–6 h and then vented in a fume hood for 2 h to remove excess OsO<sub>4</sub>. *Note: OsO<sub>4</sub> is a vigorous oxidizing agent that should be isolated from living tissue.* Cryo-TEM experiments were conducted within 7 days of staining. Stained

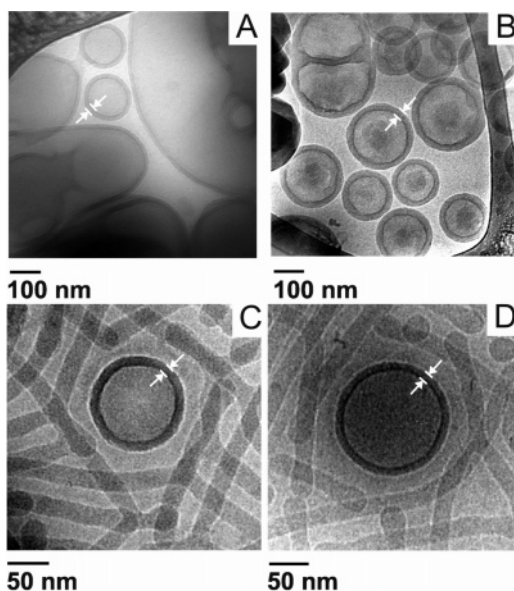


**Figure 2.** Cryo-TEM images of dilute (0.5 wt %), unstained, tetrablock copolymer aqueous dispersions: (A) OSBO-36, (B) OSBO-46, (C) OSBO-52, (D) OSBO-66. Specimens OSBO-36 and OSBO-46 produce almost exclusively vesicles with 21 nm wall thickness, while OSBO-52 and OSBO-66 contain mixed morphologies, mostly wormlike micelles and a minority of vesicles with 12 nm wall thickness. Arrows indicate wall thickness.

solutions stored for more than 2 weeks appeared to be degraded, displaying large dark aggregates when evaluated by cryo-TEM.

Cryogenic transmission electron microscopy (cryo-TEM) specimens were prepared in a controlled environment vitrification system (CEVS).<sup>33</sup> Commercially available TEM grids coated with holey carbon film (200 mesh, Ted Pella) were placed in the CEVS, and approximately 10  $\mu$ L of solution was delivered to each grid via a pipet. Excess solution was removed by blotting the grid with a small piece of filter paper, resulting in a thin film of solution (approximately 100–300 nm thick) suspended in the voids of the holey polymer film. The blotted grid was held for 30 s or more to allow recovery from the shear flow caused by blotting, and the grid was then plunged into a pool of liquid ethane at its freezing point ( $\sim -181$  °C). Vitrified grids were transferred under a nitrogen atmosphere to a liquid nitrogen cooled cryo-TEM holder (Gatan 626).

Cryo-TEM images were obtained using a JEOL 1210 TEM operated at 120 kV and equipped with a Gatan 724 multiscan digital camera. Phase contrast was enhanced by adjusting the degree of underfocus between 1 and 30  $\mu$ m. Figure 2 contains images representative of each unstained specimen. OSBO-36 and OSBO-46

form nearly exclusively vesicles, while OSBO-52 and OSBO-66, in solution, have a principal morphology of cylindrical micelles, which coexist with a minority population of vesicles.

Increasing the corona (O) block size at constant core (SB) molecular weight has three noteworthy effects on the state of dispersion. First, the average vesicle dimension and apparent size distribution decrease when  $w_O$  is increased from 36 to 46%. Although we cannot quantify this feature (due to film thickness less than the diameter of the larger vesicles), the effect is clearly evident in Figure 2A,B. Second, a morphological transition occurs between  $w_O$  of 46% and 52%. Mixed morphologies, such as those found in OSBO-52 and OSBO-66, are common in block copolymer dispersions;<sup>30</sup> this communication focuses on the vesicles. Comparison of image intensity profiles taken perpendicular to the vesicles walls reveals two core dimensions: 21 and 12 nm for  $w_O < 0.5$  and  $w_O > 0.5$ , respectively.

In comparison to the cylindrical micelles, the vesicles appeared to have a thinner hydrophobic core, even though the hydrophobic group is identical. This phenomenon, which has been documented in diblock copolymer micelles, results from chain stretching in the hydrophobic core.<sup>29</sup> Vesicle thinning reflects two effects: less crowding at a flat interface vs a concave one and the structural transition from a thick-walled bilayer to the in-plane modulated morphology.

The third effect was revealed by the stained cryo-TEM experiments as shown in Figure 3. Small OSBO-36 vesicles are characterized by two levels of core contrast: image intensity profiles reveal a 10 nm outer layer and an 11 nm inner layer, exhibiting lower and higher TEM contrast, respectively. (These experiments were only feasible with relatively small vesicles.) We associate these features with poly(styrene) and stained poly(butadiene), respectively, consistent with the 21 nm unstained membrane thickness.

OSBO-52 vesicles produced a qualitatively different result. The stained vesicle boundary measures 12 nm thick and exhibits a  $20 \pm 1$  nm azimuthally periodic variation in contrast. Moreover, the central portion of the vesicle is characterized by a subtle but distinct pattern of light and dark patches; image analysis indicates a  $20 \pm 1$  nm periodicity. Similar images were recorded for OSBO-66 vesicles, with identical periodic features, within experimental error. Addition of OsO<sub>4</sub> allowed direct visualization of the two distinct hydrophobic blocks in the micelle cores, without disrupting the overall structural characteristics of the micelles; this technique is commonly employed with SB melts. Absence of structural artifact was verified through measurement of vesicle morphology and core thickness before and after staining (not shown).

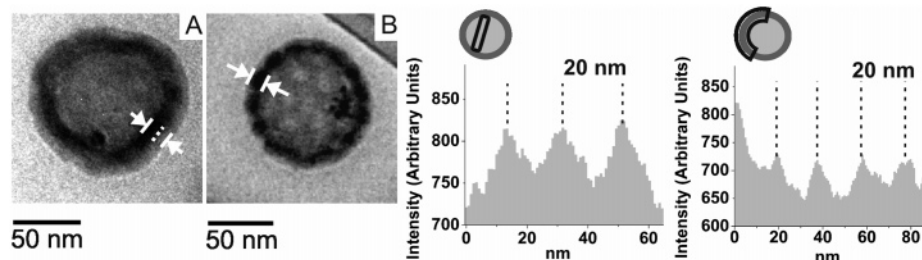


**Figure 3.** Representative cryo-TEM images of stained vesicles derived from (A) OSBO-36 and (B) OSBO-52. Arrows indicate wall thickness. In (A), a dotted line shows the vesicle wall division into a dark B layer and light S layer. Density mapping across the center and along the perimeter of (B) reveal density variations with a period of approximately 20 nm.



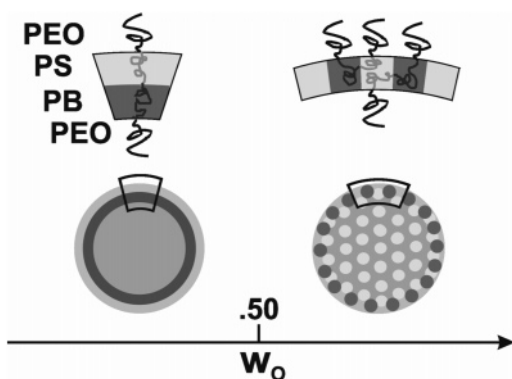


**Figure 4.** Structural models for vesicles above and below the morphological transition composition. Dark and light regions correspond to B and S regions, respectively. Cutout models of small sections of each wall type are shown above the two-dimensional projections of the complete vesicles.

We have interpreted these cryo-TEM results based on two vesicle structural models, as illustrated in Figure 4. For  $w_O \leq 0.5$  the asymmetric tetrablock architecture is manifested in a split parallel hydrophobic core, with the poly(butadiene) blocks located along the inside surface. Presumably, this broken symmetry reflects the minimization of interfacial area between water and poly(butadiene), which has a higher interfacial tension than water and poly(styrene).<sup>34</sup> This rationale also may explain the reduction in vesicle diameter in OSBO-46 relative to OSBO-36. Generation of the symmetry-breaking internal interface, in concert with poly(ethylene oxide) corona packing constraints, likely reduces the optimal vesicle size relative to conventional bilayers, where zero mean curvature (i.e., a bigger diameter) is favored.

The structure depicted in Figure 4 for  $w_O > 0.5$  is consistent with these ideas. Increasing the corona size (i.e., O block molecular weight) would reduce the vesicle diameter yet further, resulting in additional, thermodynamically unfavorable, interfacial area. Reestablishing membrane symmetry, through the creation of in-plane order, relaxes this constraint. We cannot identify the exact form of this morphology on the basis of the current cryo-TEM results. Nevertheless, a smaller membrane thickness, and comparable in-plane periodicity, suggests either a bicontinuous or hexagonally arranged state of segregation that exposes both B and S domains to inner and outer core/corona interfaces. For simplicity we have illustrated the latter arrangement in Figure 4. The transition from asymmetric bilayer to in-plane order closely resembles the lamellae-to-perforated lamellae transition reported in diblock copolymer melts.<sup>35</sup> We suspect the in-plane structured micelles are metastable relative to cylindrical micelles, locked in a kinetically trapped nonergodic state of dispersion that is likely stabilized by the glassy state of the S domains.<sup>30</sup>

This configuration is analogous to a lamellar orientation seen in diblock copolymers confined between two rigid walls<sup>36,37</sup> and in triblock copolymer thin films.<sup>38,39</sup> Under certain circumstances, these systems produce lamellae oriented perpendicular, rather than parallel, to the surface. These two lamellar orientations are superficially similar to those depicted in Figure 4, although the underlying factors responsible for these behaviors are qualitatively different.

These findings and speculations expose a new approach to designing and characterizing polymer vesicles.

Our synthetic procedure permits two additional levels of architectural symmetry breaking: OSBO', where O and O' refer to different poly(ethylene oxide) block lengths, and asymmetric core compositions. We will report on these approaches in subsequent reports. Combining classical staining techniques with cryo-TEM provides a powerful tool for characterizing the resulting structures.

**Acknowledgment.** This work was supported by NIH Grant R21 EB003164-01 (with the University of Pennsylvania) and by the Materials Research Science and Engineering Center (MRSEC) at the University of Minnesota.

## References and Notes

- (1) Yu, K.; Bartels, C.; Eisenberg, A. *Macromolecules* **1998**, *31*, 9399–9402.
- (2) Yu, K.; Eisenberg, A. *Macromolecules* **1996**, *29*, 6359–6361.
- (3) Yu, Y.; Zhang, L.; Eisenberg, A. *Langmuir* **1997**, *13*, 2578–2581.
- (4) Yu, Y.; Eisenberg, A. *J. Am. Chem. Soc.* **1997**, *119*, 8383–8384.
- (5) Shen, H.; Eisenberg, A. *Macromolecules* **2000**, *33*, 2561–2572.
- (6) Jain, S.; Bates, F. S. *Science* **2003**, *300*, 460–464.
- (7) Bermudez, H.; Brannan, A. K.; Hammer, D. A.; Bates, F. S.; Discher, D. E. *Macromolecules* **2002**, *35*, 8203–8208.
- (8) Zhang, L.; Eisenberg, A. *J. Polym. Sci., Part B: Polym. Phys.* **1999**, *37*, 1469–1484.
- (9) Maassen, H. P.; Yang, J. L.; Wegner, G. *Makromol. Chem., Macromol. Symp.* **1990**, *39*, 215–228.
- (10) Noolandi, J.; Shi, A.-C.; Linse, P. *Macromolecules* **1996**, *29*, 5907–5919.
- (11) Zhou, Z.; Chu, B. *Macromolecules* **1988**, *21*, 2548–2554.
- (12) Alexandridis, P.; Shusharina, N. P.; Yong, K.-T.; Chain, K.-K.; Balijepalli, S.; Gruenbauer, H. J. M. *Polym. Prepr. (Am. Chem. Soc., Div. Polym. Chem.)* **2003**, *44*, 218–219.
- (13) Chen, W.-Y.; Alexandridis, P.; Su, C.-K.; Patrickios, C. S.; Hertler, W. R.; Hatton, T. A. *Macromolecules* **1995**, *28*, 8604–8611.
- (14) Zhou, Z.; Li, Z.; Ren, Y.; Hillmyer, M. A.; Lodge, T. P. *J. Am. Chem. Soc.* **2003**, *125*, 10182–10183.
- (15) Yu, G.-e.; Eisenberg, A. *Macromolecules* **1998**, *31*, 5546–5549.
- (16) Gadzinowski, M.; Sosnowski, S. *J. Polym. Sci., Part A: Polym. Chem.* **2003**, *41*, 3750–3760.
- (17) Lei, L.; Gohy, J.-F.; Willet, N.; Zhang, J.-X.; Varshney, S.; Jerome, R. *Macromolecules*, in press.
- (18) Adams, M. L.; Lavasanifar, A.; Kwon, G. S. *J. Pharm. Sci.* **2003**, *92*, 1343–1355.
- (19) Discher, B. M. *Curr. Opin. Colloid Interface Sci.* **2000**, *5*.
- (20) Discher, B. M.; Won, Y.-Y.; Ege, D. S.; Lee, J. C. M.; Bates, F. S.; Discher, D. E.; Hammer, D. A. *Science (Washington, D. C.)* **1999**, *284*, 1143–1146.
- (21) Eisenberg, A.; Maysinger, D.; Allen, C. U.S. Patent 4,469,132, 2002.
- (22) Lee, J. C.; Bermudez, H.; Discher, B. M.; Sheehan, M. A.; Won, Y. Y.; Bates, F. S.; Discher, D. E. *Biotechnol. Bioeng.* **2001**, *73*, 135–145.
- (23) Photos, P. J.; Bacakova, L.; Discher, B.; Bates, F. S.; Discher, D. E. *J. Controlled Release* **2003**, *90*, 323–334.
- (24) Soo, P. L.; Terreau, O.; Savic, R.; Allen, C.; Maysinger, D.; Eisenberg, A. *Polym. Prepr. (Am. Chem. Soc., Div. Polym. Chem.)* **2000**, *41*, 1605–1606.
- (25) Erhardt, R.; Boeker, A.; Zettl, H.; Kaya, H.; Pyckhout-Hintzen, W.; Krausch, G.; Abetz, V.; Mueller, A. H. E. *Macromolecules* **2001**, *34*, 1069–1075.
- (26) Erhardt, R.; Zhang, M.; Boeker, A.; Zettl, H.; Abetz, C.; Frederik, P.; Krausch, G.; Abetz, V.; Mueller, A. H. E. *J. Am. Chem. Soc.* **2003**, *125*, 3260–3267.
- (27) Erhardt, R.; Boeker, A.; Zettl, H.; Kaya, H.; Pyckhout-Hintzen, W.; Krausch, G.; Abetz, V.; Mueller, A. H. E. *Polym. Mater. Sci. Eng.* **2001**, *84*, 102–103.
- (28) Mori, H.; Mueller, A. H. E. *Prog. Polym. Sci.* **2003**, *28*, 1403–1439.
- (29) Won, Y.-Y.; Brannan, A. K.; Davis, H. T.; Bates, F. S. *J. Phys. Chem. B* **2002**, *106*, 3354–3364.
- (30) Jain, S.; Bates, F. S. *Macromolecules* **2004**, *37*, 1511–1523.

- (31) Luo, L.; Eisenberg, A. *Langmuir* **2001**, *17*, 6804–6811.
- (32) Luo, L.; Eisenberg, A. *J. Am. Chem. Soc.* **2001**, *123*, 1012–1013.
- (33) Bellare, J. R.; Davis, H. T.; Scriven, L. E.; Talmon, Y. *J. Electron Microsc. Tech.* **1988**, *10*, 87–111.
- (34) Mark, J. E. *Polymer Data Handbook*; Oxford University Press: New York, 1999.
- (35) Hajduk, D. A.; Ho, R.-M.; Hillmyer, M. A.; Bates, F. S.; Almdal, K. *J. Phys. Chem. B* **1998**, *102*, 1356–1363.
- (36) Walton, D. G.; Kellogg, G. J.; Mayes, A. M.; Lambooy, P.; Russell, T. P. *Macromolecules* **1994**, *27*, 6225–6228.
- (37) Matsen, M. W. *J. Chem. Phys.* **1997**, *106*, 7781–7791.
- (38) Stocker, W. *Macromolecules* **1998**, *31*, 5536–5538.
- (39) Stocker, W.; Beckmann, J.; Stadler, R.; Rabe, J. P. *Macromolecules* **1996**, *29*, 7502–7507.

MA048858M